ACS Catalysis

Research Article

pubs.acs.org/acscatalysis

Use of H_2S to Probe the Active Sites in FeNC Catalysts for the Oxygen Reduction Reaction (ORR) in Acidic Media

Deepika Singh,[†] Kuldeep Mamtani,[†] Christopher R. Bruening,[†] Jeffrey T. Miller,[‡] and Umit S. Ozkan[†,*]

[†]Department of Chemical and Biomolecular Engineering, The Ohio State University, Columbus Ohio 43202, United States

[‡]Chemical Sciences and Engineering Division, Argonne National Laboratory, 9700 South Cass Avenue, Argonne, Illinois 60439, United States

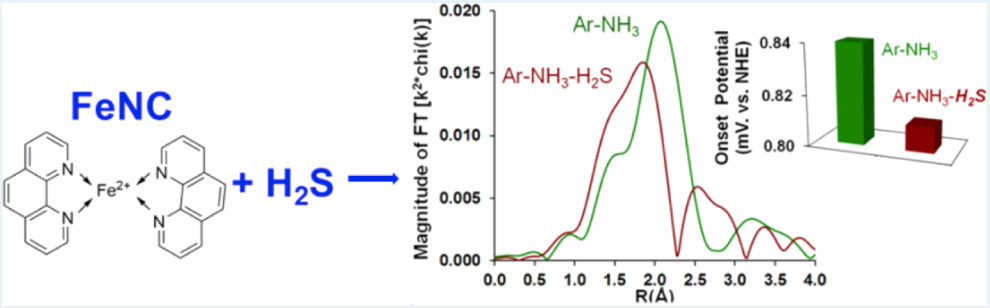

ABSTRACT: H_2S has been used as a probe molecule both in an "in situ" poisoning experiment and in intermediate-temperature heat-treatment steps during and after the preparation of FeNC catalysts in an attempt to analyze its effect on their ORR activity. The heat treatments were employed either on the ball-milled precursor of FeNC or after the Ar-NH_3 high temperature heat treatments. ORR activity of the H_2S-treated catalysts was seen to be significantly lower than the sulfur-free catalysts, whether the sulfur exposure was during a half-cell testing, or as an intermediate-temperature exposure to H_2S. The incorporation of sulfur species and interaction of Fe with sulfur were confirmed by characterization using XPS, EXAFS, TPO, and TPD. This study provides crucial evidence regarding differences in active sites in FeNC versus nitrogen-containing carbon nanostructured (CN_x) catalysts.

KEYWORDS: *H_2S, FeNC, CN_x, sulfur deactivation, ORR*

INTRODUCTION

Increasing oil prices and greenhouse emissions have led to an increased incentive toward development of alternate sources of energy and clean energy conversion devices. The hydrogen-fueled proton exchange membrane (PEM) fuel cell cars are seen as a viable alternative to automobiles powered by gasoline. The widespread use of fuel cells is, however, currently impeded by the high costs, a significant fraction of which arises from the expensive noble metal (platinum) catalyst employed for the cathodic oxygen reduction reaction (ORR). To overcome the high cost associated with platinum, non-noble metal catalysts (NNMCs) have been explored extensively as an alternative to platinum cathode catalysts in the past few decades.

NNMCs originated from metal-containing macrocyclic complexes in the mid 1960s,[1] which showed high activity for ORR in alkaline medium. It was later established that, upon a high-temperature heat treatment, a nitrogen and carbon source along with a transition metal precursor, would yield active ORR materials.[2,3] Since then, they have been prepared using numerous starting materials such as polyaniline,[4] acetonitrile,[5] ammonia[6] as nitrogen precursors, with a carbon black support such as Vulcan carbon, Ketjen Black or Black Pearls 2000, and transition metal precursors such as iron or cobalt acetate.[7,8]

Catalysts that are heat-treated in an inert or reactive gas with an existing metal−nitrogen matrix, are commonly referred to as Me(Fe or Co) NC catalysts. There is a large body of literature published by Dodelet and co-workers who conducted studies on these MeNC catalysts varying the iron and cobalt precursors,[9,10] the nitrogen sources[11] as well as carbon supports.[12,13] More recently, they replaced carbon support with a zeolitic-imidazolate framework to host the iron−nitrogen coordination.[14] They reported breakthrough catalytic activity for this formulation, making NNMCs a viable alternative to platinum in the near future. In these materials, the active site is thought to be FeN_4 or FeN_{2+2} sites hosted within the micropores of a highly microporous support.[15−17]

The existence of this active site has been confirmed more recently by Mössbauer spectroscopy revealing that Fe in its high spin state is seen to be active for ORR and an edge nitrogen group (such as a pyridinic nitrogen functionality) acts as a relay for an efficient transfer of protons for the oxygen reduction reaction to occur.[18−21] Due to different preparation

Received: May 5, 2014
Revised: July 29, 2014
Published: August 25, 2014

   dx.doi.org/10.1021/cs500612k | ACS Catal. 2014, 4, 3454−3462

parameters used for carbon-based Fe−N catalysts, there is still an ongoing debate about the active site of these materials.

A second group of materials, which are sometimes considered together with MeNC catalysts but have recently been shown to be different materials with completely different active sites,[22] are the nitrogen-containing graphitic nanostructures (CN_x). Ozkan and her group were among the first to report the use of nitrogen-doped carbon nanostructures grown on oxide supports by the decomposition of acetonitrile at high temperatures, as ORR catalysts in acidic media. In these studies, pyridinic nitrogen functional groups located on the edge of graphitic edge planes have been seen to be a marker for ORR activity in acidic media.[23−27] One possible explanation for the activity of these materials is that these functional groups (pyridinic-N) contain a lone pair of electrons, thus enhancing the electron-donating characteristics of the neighboring carbon atom, which catalyzes ORR. Iron or cobalt, if used in the preparation of these materials, serves the role of aiding catalytic formation of the active sites that consist of graphitic edge planes with pyridinic nitrogen groups.[28−30] The transition metal does not appear to participate in catalyzing ORR itself, as significant activity was obtained with CN_x catalysts grown on alumina support without a transition metal precursor used in the growth substrate.[31] When a transition metal is used as a growth catalyst, it is either encased in the carbon structures or, if exposed, is leached away together with the oxide support during an acid-washing step. More recently, work by and Dai and co-workers[32−35] on metal-free nitrogen-doped graphene with significantly high activity for ORR in alkaline media has provided more definitive evidence of the existence of such catalysts with nitrogen−carbon coordination as the active sites, instead of metal−nitrogen−carbon coordination.

In order to probe the active sites of these materials, several researchers have attempted to poison them using CO and CN^-,[36,37] with an initial hypothesis that a metal-centered active site would rapidly deactivate in the presence of these metal-binding molecules. An earlier study by Bae and Scherson conducted using in situ X-ray absorption spectroscopy indicated that CO formed an adduct with an iron porphyrin macrocycle (FeTMPP), modifying its redox cycle in the acidic medium.[38] However, it was unclear if the binding of CO to FeTMPP blocked the active site of the catalyst for ORR. More recently Dodelet and co-workers demonstrated that catalysts with possible active metal centers, such as pyrolyzed and unpyrolyzed macrocycles, did not exhibit any deactivation with CO exposure in sulfuric acid,[37] but it was suggested that this observation was not sufficient to conclude that the metal center did not play an active role in catalyzing ORR.

The first report of CN^- poisoning appeared from Yeager's group,[39] in which the researchers observed that in Co tetramethoxyphenyl porphyrins the redox couple of Co(III)/Co(II) shifted by almost 500 mV negative in the presence of CN^-, along with a negative shift for O_2 reduction by ∼120 mV. More recently, Gewirth and co-workers confirmed the poisoning effect of cyanide on pyrolyzed and unpyrolyzed macrocycles, with an evident decrease of the ORR onset potential in alkaline media, suggesting the existence of an Fe-centered active site.[36]

Poisoning studies have also been carried out recently on nitrogen-doped carbon nanostructured (CN_x) catalysts by Ozkan and co-workers.[40,41] There was a dilution effect observed for CN_x when part of O_2 was replaced by CO in the acidic media, which was no different from the effect of Ar.[40] In addition, CN_x showed no deactivation in the presence of cyanide.

More recently, we suggested that FeNC and CN_x materials may indeed be different types of ORR catalysts, with possibly different mechanisms for catalyzing the reaction.[22] FeNC catalysts contain a metal−nitrogen coordination as their active site, but this is clearly different from CN_x materials which show no indication of a metal-containing active site.[40,42]

In this study, we further examine the differences in the active sites of these materials by using H_2S as a probe molecule. In the first phase of the study, we have conducted a systematic poisoning of FeNC ORR catalysts by exposing them to H_2S at various stages of their preparation. The goal was to examine the interaction of sulfur with Fe sites and to observe any changes in the activity and coordination environment of Fe due to sulfur exposure. The treatment conditions used were identical to those used in the study performed on CN_x and Pt−C catalysts,[41] in which an evident deactivation for ORR was observed for Pt catalyst in acidic media, whereas CN_x exhibited no such deactivation.

In a separate set of experiments, in addition to the intermediate-temperature sulfur treatment, H_2S exposure was done in situ during a half-cell testing, using procedures similar to those used for the CO- and CN-poisoning experiments mentioned above. The aim of the study reported in this article is to compare the deactivation behavior of Fe−N−C with that of previously reported CN_x materials, upon contact with H_2S in a high-temperature atmosphere as well as during an ambient temperature half-cell testing and to shed light on the differences in the catalytic active sites of these materials.

EXPERIMENTAL METHODS

Catalyst Synthesis. The sulfur-free FeNC catalysts were synthesized according to the procedure discussed by Lefèvre et al.[43] Briefly, the catalyst precursor was prepared via a wet-impregnation technique by dissolving 1,10-phenanthroline (phen) in 150 mL solution of 2:1 deionized water:ethanol (200 proof, Fisher Scientific). One percent w/w of iron(II) acetate (Sigma-Aldrich) was then added to this solution, which was stirred until it achieved a deep-red color indicative of the formation of $[Fe(phen)_3]^{2+}$ complex. Black Pearls (BP) 2000 (Cabot Corp.) was added to this solution such that a ratio of 50:50 phen/BP2000 was achieved. The mixture was stirred at 70 °C until about one-third remained after evaporation. The solution was then placed overnight in a drying oven at 90 °C. The residue obtained after drying was ball-milled for 3 h in a rotary ball-mill at 200 rpm. The resulting fine powder was then weighed into a quartz boat, which was placed at the end of a long quartz tube in a pyrolysis furnace, such that the quartz boat itself was outside the furnace. The furnace was heated to 1050 °C with argon gas flowing at ∼300 mL/min, and upon reaching the set-point, the quartz boat was inserted into the furnace by means of a magnet-containing glass-rod directed by an external horseshoe magnet. The catalyst was then treated in argon for 1 h, and removed from the furnace upon completion of the treatment time. A portion of the catalyst was then subjected to a second heat treatment in NH_3 at 950 °C for 20 min, following the same procedure outlined above.

H_2S, Ar, or H_2 Treatments of Catalysts. For the H_2S or H_2 treatment of FeNC precursor or catalysts, approximately 150 mg of the catalyst was placed in a quartz boat in a high temperature furnace. The furnace was ramped up to 350 °C in 35 mL/min N_2. Once the furnace temperature reached 350 °C, the flow was switched to 35 mL/min of 500 ppm of H_2S/N_2. The catalyst was treated in H_2S or H_2 for 4h, upon which the furnace began to cool down and the gas flow was switched back to N_2. To differentiate between the poisoning effect of H_2S from its potential reducing effect, similar experiments were performed using 5% H_2/N_2 under identical conditions. The treatments

dx.doi.org/10.1021/cs500612k | ACS Catal. 2014, 4, 3454−3462

Table 1. Nomenclature of Samples Used in This Study

nomenclature used	intermediate heat treatment (350 °C, 4 h)	inert heat treatment (1050 °C, 1 h)	NH_3 heat treatment (950 °C, 20 min)	post-ammonia treatment (350 °C, 4 h)
FeNC-Ar	–	Ar	–	–
FeNC-***H_2S***-Ar	H_2S	Ar	–	–
FeNC-***Ar***-Ar	Ar	Ar	–	–
FeNC-***H_2***-Ar	H_2	Ar	–	–
FeNC-Ar-NH_3	–	Ar	NH_3	–
FeNC-Ar-NH_3-***H_2S***	–	Ar	NH_3	H_2S
FeNC-Ar-NH_3-***Ar***	–	Ar	NH_3	Ar
FeNC-Ar-NH_3-***H_2***	–	Ar	NH_3	H_2
FeNC-***H_2S***-Ar-NH_3	H_2S	Ar	NH_3	–

in H_2S or H_2 at 350 °C for 4h were employed either as an intermediate or as a terminal treatment. Ar was also used as a treatment gas at 350 °C for 4h, as a control to evaluate the effect of heat treatment without a reactive gas. The flow through the quartz tube was kept at Argon throughout the temperature ramp rate, hold time and cool down.

The catalysts prepared for this study are denoted using the nomenclature shown in Table 1.

Rotating Disk Electrode (RDE) Activity Tests. A rotating disk electrode was used to measure the electrochemical activity of the catalysts in a 0.5 M H_2SO_4 solution. The catalyst ink was prepared by dispersing 10 mg of catalyst in 95 μL of 5 wt % Nafion solution and 350 μL ethanol. The ink was sonicated in an ice bath until the catalyst was well-dispersed ($\geq$1 h), at which time 7 μL of the ink was pipetted onto a glassy carbon disk of area 0.1962 cm^2, resulting in a catalyst loading of 800 $\mu g/cm^2$. An Ag/AgCl (saturated KCl) reference electrode was used with a platinum wire as the counter electrode. Cyclic voltammograms (CVs) were first collected from 1.2 to 0.0 V to 1.2 V vs NHE at 50 mV/s in an O_2-saturated solution several times until stable CVs were obtained at 2500 rpm. Thereafter, slower CVs were collected in the same potential range at 10 mV/s to measure the activity of the catalyst. The solution was then saturated in argon, and the same procedure stated above was repeated to obtain the capacitive current for background subtraction. The activity of the catalyst was defined by the onset potential at which the background subtracted current density was equal to −0.1 mA/cm^2.

In Situ H_2S Poisoning during Rotating Disk Electrode (RDE) Activity Tests. In order to examine the interaction of H_2S with the active sites, an "in situ" poisoning experiment was performed. The goal was to provide a direct comparison to the CO or cyanide poisoning experiment reported previously. This RDE experiment was performed in 0.1 M $HClO_4$ to ensure the $SO4^{2-}$ ions in the sulfuric acid medium do not affect the results. The other experimental details are the same as those mentioned above. Briefly, CVs were collected in oxygen-saturated 0.1 M $HClO_4$ solution to determine the initial activity. Then, 500 ppm of H_2S/N_2 was bubbled through the electrolyte for 75 min while the electrode was rotated at 1000 rpm. The electrolyte was then resaturated with oxygen, and scans were collected to obtain the activity after H_2S treatment.

X-ray Photoelectron Spectroscopy (XPS). XPS was used to analyze the composition of the surface species present on the FeNC catalysts. A Kratos Ultra Axis spectrometer was used with a monochromated aluminum anode source operated at 12 kV and 10 mA. Collected data were corrected for charge shifting using standard C 1s binding energy of 284.5 eV. XPS Peak 4.1 software package was used for curve fitting. Spectra baselines were determined using Shirley-type background fitting. Spectra were deconvoluted using Lorentzian–Gaussian combination peaks.

Temperature-Programmed Oxidation (TPO) and Temperature-Programmed Desorption (TPD) experiments. TPO experiments were performed using 7 mg of catalyst loaded into a 4-mm ID quartz reactor with a quartz frit, heated in a Carbolite, MTF 10/15/30 furnace under 5% O_2/N_2 at 30 ccm, with a linear temperature program ramp rate of 10 °C/min up to 900 °C. The TPO product stream was fed to an MKS Cirrus benchtop residual gas analyzer with mass signals of 1–100 monitored throughout the experiment. TPD experiments were performed by using the same parameters as those for the TPO experiments under pure He at 30 ccm.

X-ray Absorption Fine Structure Spectroscopy. Spectra were collected for the Fe K edge (7112 eV) at the bending magnet beamline (5BM-D) of the Dow-Northwestern-DuPont Collaborative Access Team (DND-CAT) of the Advanced Photon Source, Argonne National Laboratory. The measurements were made in transmission mode with the Si(111) monochromator detuned by 30% to eliminate the higher-order harmonics in the beam. The samples were pelletized using a die of diameter 13 mm and held in a six sample-holder against Kapton tapes transparent to the X-ray beam. There was no binder used to dilute the samples further, as the iron concentrations were low to begin with. All samples and standards were collected in the ex situ mode.

RESULTS AND DISCUSSION

Rotating Disk Electrode Experiments. ORR RDE scans collected in 0.5 M H_2SO_4 solutions for FeNC-Ar-NH_3 (standard FeNC catalyst in its most active form), and the samples that went through H_2S, H_2, or Ar treatment (FeNC-Ar-NH_3-***H_2S***, FeNC-Ar-NH_3-***H_2***, and FeNC-Ar-NH_3-***Ar***) and are shown in Figure 1. The rationale for using the latter treatments was to differentiate between the poisoning effect of H_2S and the effect of a post-ammonia treatment with a nonreacting gas such as Ar or a reducing gas such as H_2. It is evident that, while Fe-N-C-Ar-NH_3, FeNC-Ar-NH_3-***Ar*** and FeNC-Ar-NH_3-***H_2*** have nearly identical onset potentials (0.84 V), the onset potential for FeNC-Ar-NH_3-***H_2S*** is lower by 30

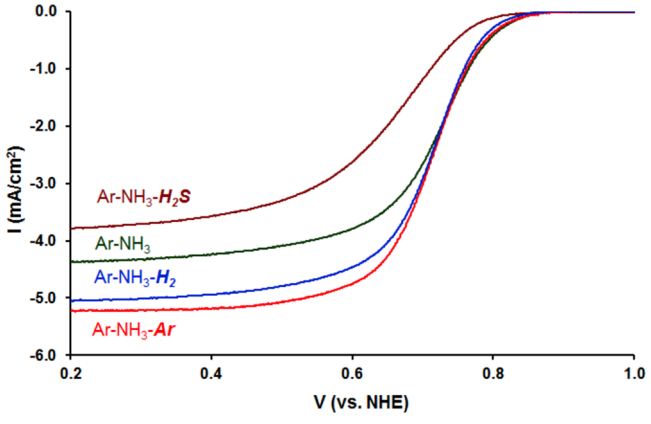

Figure 1. ORR activity measurements by RDE in 0.5 M H_2SO_4 at 2500 rpm. Effect of treatment with H_2S, H_2, or Ar after high-temperature Ar-NH_3 treatment.

dx.doi.org/10.1021/cs500612k | ACS Catal. 2014, 4, 3454–3462

mV. The control experiments with Ar and H_2 show that the activity loss is not due to a heat treatment effect or reduction effect. These results indicate that FeNC catalyst suffers from a pronounced activity loss after H_2S treatment, which cannot be explained by a post-ammonia inert heat treatment effect or a reduction effect.

We also compared the effect of sulfur treatment on a FeNC-precursor, Black Pearls impregnated with 1,10-phenanthroline and iron(II) acetate solution and ball-milled prior to any high-temperature heating. The sample was treated in H_2S/N_2 at 350 °C for 4 h, followed by Ar treatment at 1050 °C for 1 h. The ORR RDE scans for FeNC-***H_2S***-Ar and FeNC-Ar are shown in Figure 2. There was a pronounced deactivation effect observed

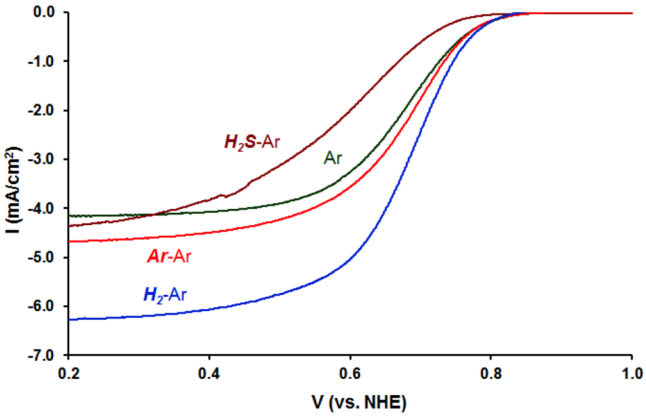

Figure 2. ORR activity measurements by RDE in 0.5 M H_2SO_4 at 2500 rpm. Effect of low-temperature-treatment with H_2S, H_2, or Ar before high-temperature Ar treatment.

with the H_2S treatment, such that FeNC-***H_2S***-Ar showed a lower onset of activity by 40 mV than the catalyst prepared by treatment in Ar only (FeNC-Ar). This deactivation effect was exclusive to exposure to H_2S. We performed control experiments by using H_2 or Ar instead of H_2S (FeNC-***H_2***-Ar and FeNC-***Ar***-Ar) in order to eliminate the effect of a low-temperature heat treatment, or an exposure to a reducing environment prior to a high-temperature treatment and saw that the deactivation was not observed with either of the two gases, and was seen with H_2S only.

In Figure 3, we compare the ORR activities of FeNC-***H_2S***-Ar-NH_3, FeNC-Ar-NH_3-***H_2S*** with FeNC-Ar-NH_3 catalyst, to evaluate the effect of H_2S treatments at two different stages, i.e., before any heat treatment and after Ar and NH_3 treatments. It is observed that, regardless of whether the catalyst is exposed to H_2S before the heat treatments or after, exposure to H_2S deactivates it to the same extent and significantly lowers its activity in comparison to the standard and most active form of the catalyst, FeNC-Ar-NH_3.

It should also be noted that the differences in the limiting current densities could be caused due to changes in the surface functionalities of these catalysts, as a result of varying the sequence of heat treatments. These effects could alter the hydrophobicity of the catalysts, causing differences in the three-phase boundary within the pores of the catalyst, which in turn could affect the limiting current densities obtained. It is also conceivable that some of the heat treatments may have an "etching" effect, increasing the surface coarseness, leading to higher limiting currents.

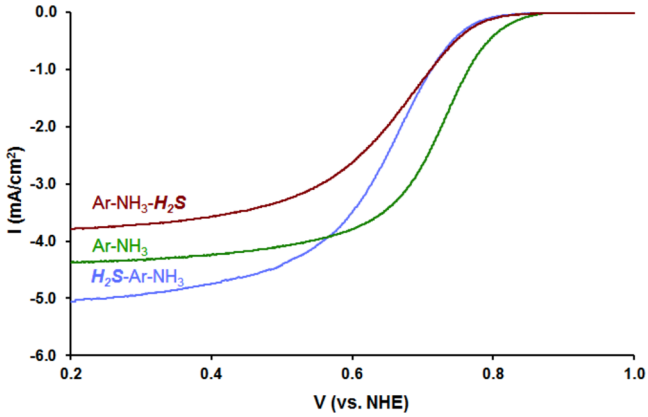

Figure 3. ORR activity measurements by RDE in 0.5 M H_2SO_4 at 2500 rpm. Effect of H_2S exposure at two different stages (pre-Ar and post-NH_3 treatment).

In Situ H_2S Poisoning during RDE Activity Tests. Figure 4 presents the RDE scans collected through an in situ

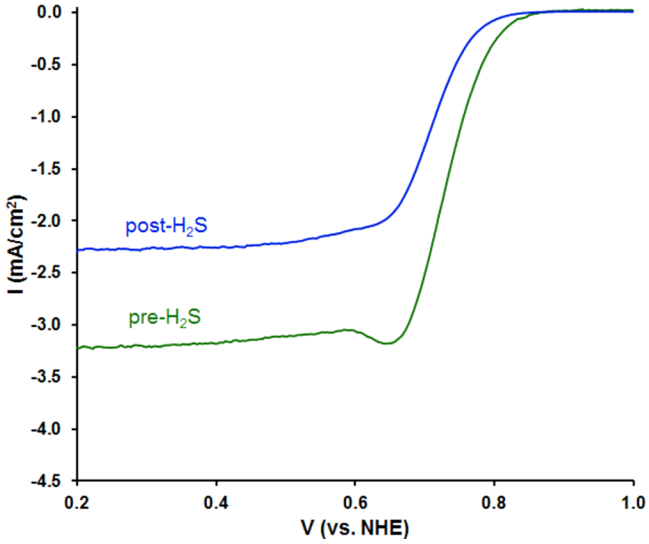

Figure 4. ORR activity measurements of FeNC-Ar-NH_3 by RDE in oxygen-saturated 0.1 M $HClO_4$ before and after in situ H_2S exposure at 1000 rpm.

poisoning experiment. In this test, the pre-H_2S scan was collected in an O_2-saturated 0.1 M $HClO_4$ solution to determine the initial activity. After bubbling 500 ppm of H_2S/N_2 through the electrolyte for 75 min while the electrode was rotated at 1000 rpm, electrolyte was then resaturated with oxygen to obtain the post-H_2S treatment. The comparison shows a net loss of activity as indicated by the decreased onset potential and the decreased limiting current. This result provides a clear evidence of the poisoning effect of H_2S on FeNC catalysts.

Temperature-Programmed Oxidation (TPO). TPO experiments were conducted for the regular and H_2S treated FeNC catalysts. Figure 5 shows a comparison of the TPO profiles for samples that have gone through different temperature and/or gas treatments.

One of the most striking features is the change in the oxidation onset temperatures for these samples upon exposure to sulfur. Since iron catalyzes the oxidation of carbon, its

dx.doi.org/10.1021/cs500612k | ACS Catal. 2014, 4, 3454−3462

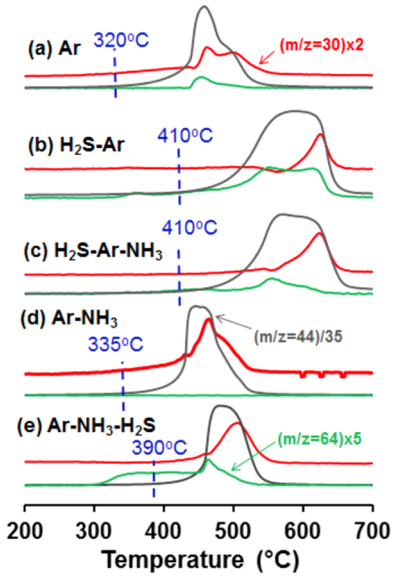

Figure 5. TPO profiles for FeNC samples that have gone through different heat and gas treatments.

presence in FeNC samples is expected to lower the oxidation onset temperature. In FeNC-Ar, oxidation starts at ∼320 °C as seen with the rise of the (m/z = 44) CO_2 signal (Figure 5a). An H_2S exposure before Ar treatment raises the oxidation onset temperature by about 90 °C (Figure 5b). This result is significant in suggesting that the Fe sites poisoned by sulfur can no longer catalyze the oxidation reaction effectively. When the FeNC-$\boldsymbol{H_2S}$-Ar sample goes through a high-temperature NH_3 treatment, this activity is not recovered, and the oxidation onset temperature does not change (Figure 5c).

For FeNC-Ar-NH_3, the oxidation onset temperature is seen to be about 335 °C (Figure 5d). Exposure to H_2S increases the oxidation onset temperature (Figure 5e), but the change is not as drastic as it was for the FeNC-$\boldsymbol{H_2S}$-Ar sample. This observation suggests that the coordination of sulfur on Fe sites may be different, depending on whether the sulfur exposure takes place before any heat treatment or after Ar-NH_3 treatment, although both of the exposure processes result in a similar extent of activity loss, as seen in the previous section (Figure 3).

In addition to CO_2, there are also nitrogen oxide species (m/z = 30) that evolve from the samples during TPO. They appear at higher temperatures than CO_2, suggesting that they are not primarily on the surface coordinated to carbon, but also in the bulk and coordinated to Fe. In sulfur-exposed samples (Figure 5 b and c), emergence of NO_x species shifts to higher temperatures, following a trend similar to that of CO_2.

A third group of species that evolve during TPO are the SO_x species (m/z = 64). They are most pronounced in FeNC-$\boldsymbol{H_2S}$-Ar (Figure 5b). They reduce significantly in FeNC-$\boldsymbol{H_2S}$-Ar-NH_3, but do not disappear altogether (Figure 5c). FeNC-Ar-NH_3-$\boldsymbol{H_2S}$ also shows SO_x species evolving during TPO, but the signal is lower than that seen over the FeNC-H_2S-***Ar*** sample.

It is interesting to note that the FeNC-Ar catalyst, which was not subjected to any prior sulfur treatment, also showed sulfur species evolving together with CO_2 (Figure 5a). This is somewhat expected, as the carbon support itself (Black Pearls 2000) has some extent of sulfur impurities embedded within its matrix.

X-ray Photoelectron Spectroscopy (XPS). *S 2p.* The S 2p region of all the H_2S-treated catalysts was scanned to identify detectable surface species. Figure 6 shows the S 2p spectra of FeNC-$\boldsymbol{H_2S}$-Ar, $\boldsymbol{H_2S}$-Ar-NH_3, and Ar-NH_3-$\boldsymbol{H_2S}$.

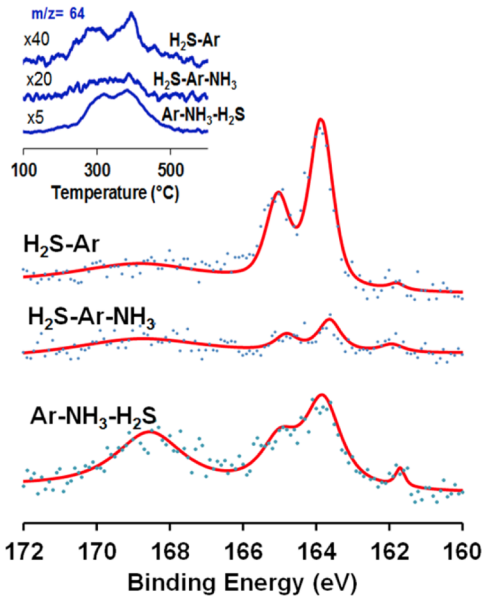

Figure 6. S 2p XPS spectra of FeNC samples that have gone through different heat and gas treatments. (Inset: TPD profiles after different heat and gas treatments.)

Three different types of sulfur species have been identified on the surface of these catalysts. There is some extent of ambiguity in the literature with peak assignments of sulfur species between 163 and 164 eV. S−C species have been reported to appear at 163, 163.6, and 163.8 eV, while 163.6 eV has also been assigned to only S−S species.[44−46] At higher BEs of ∼164.8 eV, unbound thiols and disulfides have been reported in literature,[47,48] which is very close to the value observed at 165 eV in this study. Hence, it is very likely that both S−C and S−S type species exist for these three catalysts, $\boldsymbol{H_2S}$-Ar, Ar-NH_3-$\boldsymbol{H_2S}$, and $\boldsymbol{H_2S}$-Ar-NH_3. The peaks for FeNC-$\boldsymbol{H_2S}$-Ar-NH_3 are smaller, as the two subsequent heat treatments reduce the surface sulfur species. The peak at 168.6 eV for this catalyst may be attributed to iron sulfate species.[49] It is possible that the elemental sulfur present on the surface undergoes some degree of surface oxidation, reacting with air to form sulfate species. There is also a small peak at 161.7 eV for all three catalysts, which is likely to be an Fe−S_2/Fe−S-type species.[50] The resolution of the sulfur species was not sufficiently high for data deconvolution.

The inset shows the temperature-programmed desorption profiles of SO_x species (m/z = 64) for FeNC-Ar-NH_3-$\boldsymbol{H_2S}$, $\boldsymbol{H_2S}$-Ar-NH_3, and $\boldsymbol{H_2S}$-Ar. All three catalysts showed significant evolution of SO_x species between the temperatures of 250 °C to 450 °C, confirming the existence of surface sulfur species.

Fe 2p. Fe 2p XPS spectra for FeNC-Ar and $\boldsymbol{H_2S}$-Ar are shown in Figure 7. The spectra have poor signal-to-noise ratio, possibly due to the location of Fe species inside the micropores. The peak appearing at 710 eV or higher for Fe $2p_{3/2}$ are related to Fe^{2+} or Fe^{3+} species.[51−53] This could be due to nitridic Fe species;[52] however, contribution from a thin oxide layer that could form over the exposed Fe species is also a possibility. For the sample which is exposed to H_2S, there is a distinct peak

dx.doi.org/10.1021/cs500612k | ACS Catal. 2014, 4, 3454−3462

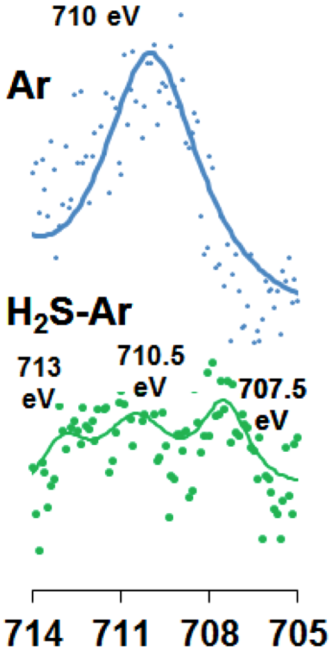

Figure 7. Fe 2p $_{3/2}$ XPS spectra of FeNC-Ar and ***H₂S***-Ar.

appearing at ~707.5 eV which could be due to FeS_2.[49] Ferrous and ferric sulfate species are also reported at 711 and 713.2 eV,[49] which are present in the ***H₂S***-Ar sample as broad contributions from multiple peaks in this range. This supports the XPS spectral analysis from S 2p region.

N 1s. The nitrogen 1s XPS spectra were deconvoluted to reveal differences in the nitrogen surface species as a function of the treatment and are plotted in Figure 8 and tabulated in Table 2.

The three main surface groups found were pyridinic-N (398.5−398.7 eV), quarternary-N (401−401.2 eV), and

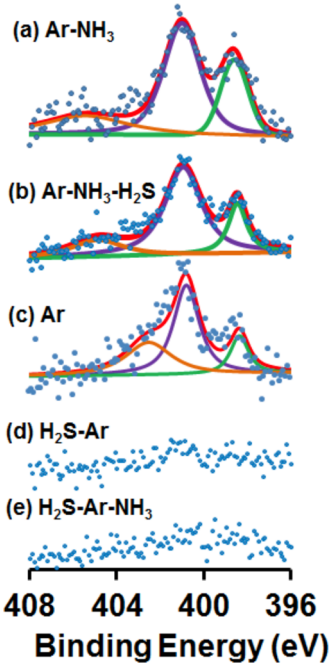

Figure 8. N 1s XPS spectra of FeNC-Ar-NH_3, Ar-NH_3-H_2S, Ar, ***H₂S***-Ar, and H_2S-Ar-NH_3.

pyridinic N^+O^- species at a higher binding energy between 402 and 405 eV.[26] Fe-coordinated nitrogen species may also be expected to have binding energies in this envelope, but these species have been reported in a wide eV range (397.3−399.7 eV),[22,54] making definitive assignments difficult.

It should be noted that even the samples that have not gone through NH_3 treatment show the same types of nitrogen species, resulting from the treatment of the carbon support with phenanthroline. Another observation for the spectra of samples before and after NH_3 treatment (Figure 8 a and c) is that pyridinic-N species have become more pronounced after the ammonia treatment. The prominent presence of pyridinic-N species in these catalysts may suggest two types of active sites, one with an Fe center, and one associated with N-groups on the carbon surface. The pyridinic nitrogen content for FeNC-Ar-NH_3-***H₂S*** is seen to be significantly lower as compared to that of FeNC-Ar-NH_3 (15% versus 25% of the total nitrogen composition), as seen in Figure 8 and Table 2. If the activity of FeNC indeed has contributions from two different types of sites, the decrease in activity of FeNC-Ar-NH_3-***H₂S*** as compared to its control can partially be due to the loss of pyridinic N sites. It is also possible that the reason for deactivation is the adsorption of sulfur onto the Fe catalytic sites via a substitution mechanism by which sulfur replaces some nitrogen functionalities coordinated to iron. This could prevent the formation of some active Fe−N_x species that catalyze ORR, leading to inhibition of activity of these catalysts.

Another important observation in Figure 8 is that, for the samples that have been exposed to H_2S prior to any high-temperature heat treatment (Figure 8 d and e), spectral features due to nitrogen species are indiscernible. It appears that H_2S exposure before any heat treatment may be leading to exchange of nitrogen groups with sulfur groups and severely impedes the formation of nitrogen surface species in the subsequent NH_3 treatments at high temperatures. The sulfur species observed in the S 2p and Fe 2p spectra support this assertion. This observation is also consistent with the detrimental effect of H_2S treatment seen on ORR activity for FeNC-***H₂S***-Ar and FeNC-***H₂S***-Ar-NH_3 samples.

EXAFS and XANES Spectra. The magnitudes of the k^2-weighted Fourier transforms (uncorrected values) for H_2S-treated FeNC catalysts were compared with their sulfur-free counterparts in Figures 9 and 10. EXAFS data for these catalysts were also fitted with reference spectra of iron sulfide, oxide, and carbide. All the values of bond distances discussed below are uncorrected values, with the correction for the E_0 shift reported in Table 3.

The magnitudes of the k^2-weighted Fourier transforms (uncorrected values) for H_2S-treated FeNC catalysts were compared with their sulfur-free counterparts in Figures 9 and 10. EXAFS data for these catalysts were also fitted with reference spectra of iron sulfide, oxide and carbide. All the values of bond distances discussed below are uncorrected values, with the correction for the E_0 shift reported in Table 3.

Figure 9 shows comparisons of (a) uncorrected FT Magnitudes and (b) XANES spectra for FeNC-Ar-NH_3-***H₂S*** with the control catalyst FeNC-Ar-NH_3 and reference iron(II) sulfide. FeNC-Ar-NH_3-***H₂S*** showed contributions from Fe−S at an uncorrected value of 1.9 Å corresponding to a bond length of 2.2 Å from the EXAFS fit (Figure 9a).[55] This is indicative of iron−sulfur bond formation, which was also seen in XPS analysis of S 2p spectra. A secondary feature at the uncorrected value of 1.4 Å may be assigned to Fe−N or Fe−O species. This

dx.doi.org/10.1021/cs500612k | ACS Catal. 2014, 4, 3454−3462

Table 2. N 1s Distribution from XPS

	percentage distribution (%)		
sample	pyridinic (398.5−398.7 eV)	quarternary (401−401.2 eV)	pyridinic N^+O^- (402−405 eV)
FeNC-Ar	16	51	33
FeNC-Ar-NH_3	25	57	18
FeNC-Ar-NH_3-H_2S	15	75	10

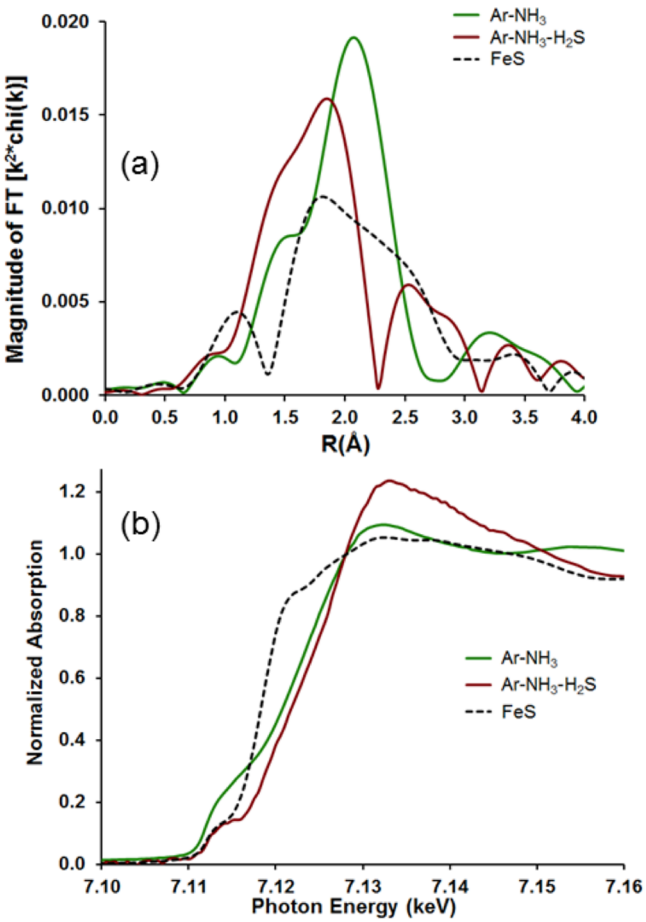

Figure 9. Fe K edge XAS spectra for FeNC-Ar-NH_3 and FeNC-Ar-NH_3-H_2S. (a) EXAFS and (b) XANES. The reference spectra for FeS is also included for comparison.

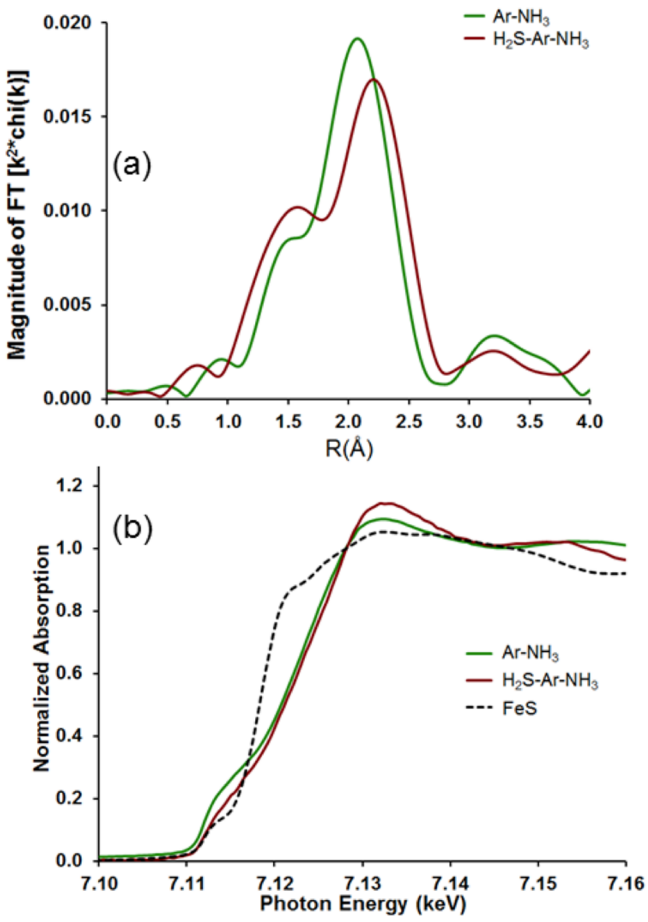

Figure 10. Fe K edge XAS spectra for FeNC-Ar-NH_3 and FeNC-H_2S-Ar-NH_3. (a) EXAFS and (b) XANES. The reference spectra for FeS is also included for comparison.

catalyst exhibits a very different coordination state from FeNC-Ar-NH_3, which shows a large peak at 2.1 Å for Fe−Fe bond present in metal carbide (2.46 Å in the EXAFS fit), with a shoulder for Fe−C appearing at 1.5 Å (2.0 Å in the EXAFS fit). This feature may have contributions from Fe−N as well.[56−58]

From the XANES spectra shown in Figure 9b, the differences in pre-edge energies are evident in the H_2S-treated and sulfur-free catalysts. While FeNC-Ar-NH_3-H_2S has a pre-edge feature identical to that of iron(II) sulfide, indicating a +2 oxidation state, it is significantly different from that of FeNC-Ar-NH_3, which shows a more metallic character. Both the XANES and EXAFS spectra imply that the sulfur treatment brought about a pronounced change in the oxidation state as well as local bonding environment of FeNC-Ar-NH_3-H_2S.

The local coordination environment of FeNC-H_2S-Ar-NH_3 was harder to interpret (Figure 10), due to the increased possibility of different contributions from nitride, carbide, or sulfide phases. The shoulder seen in the FT-magnitude plot at an uncorrected value of 1.45 Å (1.9 Å in the EXAFS fit) is likely due to Fe−O or Fe−N species. Fe appears to be in a +2 oxidation state in this catalyst. Since all of the samples are exposed to air after H_2S treatment, exchange of sulfur species with oxygen species is a possibility.

The larger peak seen in this catalyst is shifted to a slightly higher bond distance (uncorrected ∼2.2 Å) than the metallic Fe−Fe peak seen in FeNC-Ar-NH_3. This is likely due to the Fe−X−Fe scatter from a higher shell, where X could be O, C or N. It should also be noted that the light scatterers such as oxygen, nitrogen, and carbon as neighbors to the central scattering atom are hard to distinguish due to their similar electronic configurations, thus making exact interpretations of EXAFS spectra difficult. The XANES spectrum FeNC-H_2S-Ar-NH_3 is not similar to iron(II) sulfide (Figure 10b), while the pre-edge feature for this catalyst lies in between those of FeNC-Ar-NH_3 and iron(II) sulfide. As seen from the XPS data, subsequent NH_3 treatment decreases the sulfur groups on the surface. This points to the likelihood of the exchange of sulfur groups in this catalyst with some nitrogen functionalities, upon

dx.doi.org/10.1021/cs500612k | ACS Catal. 2014, 4, 3454−3462

Table 3. Results of EXAFS fits

sample	pre-edge energy, eV	edge energy, eV	scatter	N	R, Å	$\Delta\sigma^2$ ($\times 10^3$)	E_0, eV
Fe Foil		7112.0	Fe−Fe	8	2.48		
FeO	7113.1						
FeS	71129		Fe−S	4	2.23		
			Fe−Fe	4	2.59		
$Fe(AcAc)_3$	71143		Fe−O	6	1.99		
FeNC-Ar-NH_3		7112.0	Fe−Fe	4.5	2.46	3.0	−11.2
			Fe−C (or Fe−N)	2.0	2.25	2.0	−10.1
Fe−Ar−NH_3-***H_2S***	7113.3		Fe−O (or Fe−N)	1.9	1.91	1.0	−0.5
			Fe−S	3.9	2.20	1.0	8.1
FeNC-***H_2S***-Ar-NH_3	7113.1		Fe−O (or Fe−N)	3.9	1.92	8.0	12.9

subsequent NH_3 treatment. This exchange may not necessarily be complete, nor is it indicative of the formation of those specific Fe−N_x moieties found in the sulfur-free samples, which contribute to ORR activity. This is also evident in the TPO results shown in Figure 5, where evolution of m/z = 30 (NO_x) species is very different for the FeNC-***H_2S***-Ar-NH_3-treated catalyst from the sulfur-free Ar-NH_3 catalyst. Hence, even if Fe−N coordinations exist in these H_2S-treated catalysts, they may not be contributing to ORR activity. A number of studies performed recently have acknowledged the existence of multiple Fe−N_x sites in these FeNC catalysts[18,59] using Mössbauer spectroscopy which may be in a high-spin or a low-spin state, not all of which are attributed to ORR activity. Since EXAFS is limited in its capability to distinguish between the iron−nitrogen coordination specific to the spin state of iron, the presence of Fe−N_x species identified by this technique is not a direct evidence of high ORR activity in a catalyst. Nevertheless, the differences due to sulfur exposure both in coordination environment as well as activity are quite evident.

CONCLUSIONS

The H_2S heat-treatments were employed on FeNC catalysts in two steps, either (i) after the terminal heat-treatment with Ar and NH_3, or (ii) on the ball-milled precursor prior to any high-temperature treatment.

Exposure to H_2S caused significant deactivation for ORR for FeNC catalysts, when used after Ar-NH_3 treatments, an effect not observed for H_2 or Ar treatments when used instead of H_2S. These findings show that the activity loss was due to sulfur binding to the metallic center or replacing the surface functional groups and was not caused by a heat treatment in an inert or in a reducing atmosphere. Strong interaction of sulfur with FeNC surfaces was verified by catalyst characterization experiments such as TPO, EXAFS and XPS and TPD. TPO profiles indicated the presence of surface sulfur species, and the oxidation of carbon was shifted to a higher temperature, indicating that the Fe sites that catalyze carbon oxidation as well as ORR were rendered inactive with the H_2S treatment. EXAFS revealed a change in the coordination environment of Fe, after the H_2S treatment, which may have arisen from the formation of Fe−S bonds. XPS helped identify S−S or S−C surface species, along with the possibility of Fe−S-type bonds, indicating that the sulfur indeed binds to Fe in this catalyst. Another effect of the H_2S exposure after Ar-NH_3 terminal heat treatments was that it led to lower incorporation of pyridinic-N, which could also contribute to the loss of ORR activity.

When the H_2S treatment was employed on the FeNC precursor, it also lowered the catalyst's ORR activity. The absence of nitrogen species in this catalyst, even after the subsequent heat treatments with NH_3, suggests that the H_2S treatment prior to high-temperature treatments interferes with Fe−N_x site formation, which may adversely affect its activity.

A more direct evidence of the poisoning effect of sulfur on FeNC catalysts was acquired through an in situ poisoning experiment where H_2S exposure took place during an RDE experiment. The RDE scans before and after sulfur exposure showed a pronounced decrease in onset potential and in the limiting current, indicating a net decrease in the available active sites for ORR. The deactivation of FeNC catalysts seen due to exposure to H_2S is a clear indication of the role played by Fe in catalyzing ORR in these catalysts. The mechanism of deactivation may be different, depending on whether the H_2S exposure is performed on the FeNC precursor before any heat treatments, or the active form of the FeNC catalyst after the Ar-NH_3 treatment. In the former, H_2S appears to interfere with the formation of catalytically active Fe−N_x sites in the subsequent high-temperature heat treatments and in the latter, there appears to be a direct bonding of S to the Fe center as well as loss of some of the nitrogen moieties. The in situ H_2S exposure during an RDE scan at room temperature suggests adsorption of the poison on the Fe active sites.

These results are significant in highlighting the differences between FeNC and CN_x catalysts in the terms of the role of iron in their active sites for ORR. In our previous studies, we observed no detrimental effect of H_2S on CN_x, while it deactivated platinum/carbon catalyst for ORR quite readily.[41] By demonstrating that H_2S has a negative effect on ORR activity of FeNC catalysts, we provide concrete evidence that, while Fe plays a critical role in catalyzing ORR for FeNC, it does not participate in catalyzing ORR in CN_x, thereby proving that the two catalysts are indeed different classes of materials with different active sites for oxygen reduction.

AUTHOR INFORMATION

Corresponding Author

*Phone: 614-292-6623. E-mail: ozkan.1@osu.edu.

Notes

The authors declare no competing financial interest.

ACKNOWLEDGMENTS

We gratefully acknowledge the financial support by the U.S. Department of Energy, Office of Science, Office of Basic Energy Sciences, under Contract No. DE-FG02-07ER15896. Portions of this work were performed at the DuPont-Northwestern-Dow Collaborative Access Team (DND-CAT) located at Sector 5 of the Advanced Photon Source (APS). DND-CAT is supported by E.I. DuPont de Nemours and Co., The Dow Chemical

Company, and Northwestern University. Use of the APS, an Office of Science User Facility operated for the U.S. Department of Energy (DOE) Office of Science by Argonne National Laboratory, was supported by the U.S. DOE under Contract No. DE-AC02-06CH11357.

REFERENCES

(1) Jasinski, R. *Nature* **1964**, *201*, 1212−1213.
(2) Gupta, S.; Tryk, D.; Bae, I.; Aldred, W.; Yeager, E. *J. Appl. Electrochem.* **1989**, *19*, 19−27.
(3) Wiesener, K. *Electrochim. Acta* **1986**, *31*, 1073−1078.
(4) Alonso-Vante, N.; Cattarin, S.; Musiani, M. *J. Electroanal. Chem.* **2000**, *481*, 200−207.
(5) Fournier, J.; Lalande, G.; Cote, R.; Guay, D.; Dodelet, J. P. *J. Electrochem. Soc.* **1997**, *144*, 218−226.
(6) Faubert, G.; Côté, R.; Dodelet, J. P.; Lefèvre, M.; Bertrand, P. *Electrochim. Acta* **1999**, *44*, 2589−2603.
(7) Chen, Z.; Higgins, D.; Yu, A.; Zhang, L.; Zhang, J. *Energy Environ. Sci.* **2011**, *4*, 3167−3192.
(8) Jaouen, F.; Proietti, E.; Lefevre, M.; Chenitz, R.; Dodelet, J. P.; Chung, H. T.; Johnston, C. M.; Zelenay, P. *Energy Environ. Sci.* **2011**, *4*, 114−130.
(9) Dignard-Bailey, L.; Trudeau, M. L.; Joly, A.; Schulz, R.; Lalande, G.; Guay, D.; Dodelet, J. P. *J. Mater. Res.* **1994**, *9*, 3203−3209.
(10) Lalande, G.; Faubert, G.; Cote, R.; Guay, D.; Dodelet, J. P.; Weng, L. T.; Bertrand, P. *J. Power Sources* **1996**, *61*, 227−237.
(11) Cote, R.; Lalande, G.; Guay, D.; Dodelet, J. P.; Denes, G. *J. Electrochem. Soc.* **1998**, *145*, 2411−2418.
(12) Wang, H.; Cote, R.; Faubert, G.; Guay, D.; Dodelet, J. P. *J. Phys. Chem. B* **1999**, *103*, 2042−2049.
(13) Proietti, E.; Dodelet, J. P. *ECS Trans.* **2008**, *16*, 393−404.
(14) Proietti, E.; Jaouen, F.; Lefevre, M.; Larouche, N.; Tian, J.; Herranz, J.; Dodelet, J. P. *Nat. Commun.* **2011**, *2*, 416−424.
(15) Jaouen, F.; Lefevre, M.; Dodelet, J.-P.; Cai, M. *J. Phys. Chem. B* **2006**, *110*, 5553−5558.
(16) Jaouen, F.; Dodelet, J.-P. *Electrochim. Acta* **2007**, *52*, 5975−5984.
(17) Lefevre, M.; Dodelet, J.-P. *Electrochim. Acta* **2008**, *53*, 8269−8276.
(18) Kramm, U. I.; Herranz, J.; Larouche, N.; Arruda, T. M.; Lefevre, M.; Jaouen, F.; Bogdanoff, P.; Fiechter, S.; Abs-Wurmbach, I.; Mukerjee, S.; Dodelet, J. P. *Phys. Chem. Chem. Phys.* **2012**, *14*, 11673−11688.
(19) Kramm, U. I.; Abs-Wurmbach, I.; Herrmann-Geppert, I.; Radnik, J.; Fiechter, S.; Bogdanoff, P. *J. Electrochem. Soc.* **2011**, *158*, B69−B78.
(20) Ferrandon, M.; Kropf, A. J.; Myers, D. J.; Artyushkova, K.; Kramm, U.; Bogdanoff, P.; Wu, G.; Johnston, C. M.; Zelenay, P. *J. Phys. Chem. C* **2012**, *116*, 16001−16013.
(21) Muller, K.; Richter, M.; Friedrich, D.; Paloumpa, I.; Kramm, U. I.; Schmeiser, D. *Solid State Ionics* **2012**, *216*, 78−82.
(22) Singh, D.; Tian, J.; Mamtani, K.; King, J. C.; Miller, J. T.; Ozkan, U. *J. Catal.* **2014**, *317*, 30−43.
(23) Matter, P. H.; Wang, E.; Arias, M.; Biddinger, E. J.; Ozkan, U. S. *J. Mol. Catal.* **2007**, *264*, 73−81.
(24) Matter, P. H.; Wang, E.; Ozkan, U. S. *J. Catal.* **2006**, *243*, 395−403.
(25) Matter, P. H.; Wang, E.; Arias, M.; Biddinger, E. J.; Ozkan, U. S. *J. Phys. Chem. B* **2006**, *110*, 18374−18384.
(26) Matter, P. H.; Zhang, L.; Ozkan, U. S. *J. Catal.* **2006**, *239*, 83−96.
(27) Biddinger, E. J.; Ozkan, U. S. *J. Phys. Chem. C* **2010**, *114*, 15306−15314.
(28) Singh, D.; Soykal, I. I.; Tian, J.; Von Deak, D.; King, J. C.; Miller, J. T.; Ozkan, U. S. *J. Catal.* **2013**, *304*, 100−111.
(29) Matter, P. H.; Wang, E.; Millet, J.-M. M.; Ozkan, U. S. *J. Phys. Chem. C* **2007**, *111*, 1444−1450.
(30) Biddinger, E. J.; von Deak, D.; Ozkan, U. S. *Top. Catal.* **2009**, *52*, 1566−1574.
(31) Matter, P. H.; Ozkan, U. S. *Catal. Lett.* **2006**, *109*, 115−123.
(32) Gong, K.; Du, F.; Xia, Z.; Durstock, M.; Dai, L. *Science* **2009**, *323*, 760−764.
(33) Qu, L.; Yong, L.; Baek, J.-B.; Dai, L. *ACS Nano* **2010**, *4*, 1321−1326.
(34) Yu, D.; Nagelli, E.; Du, F.; Dai, L. *J. Phys. Chem. Lett.* **2010**, *1*, 2165−2173.
(35) Zhang, L.; Niu, J.; Dai, L.; Xia, Z. *Langmuir* **2012**, *28*, 7542−7550.
(36) Thorum, M. S.; Hankett, J. M.; Gewirth, A. A. *J. Phys. Chem. Lett.* **2011**, *2*, 295−298.
(37) Birry, L.; Zagal, J. H.; Dodelet, J. P. *Electrochem. Commun.* **2010**, *12*, 628−631.
(38) Bae, I. T.; Scherson, D. *J. Phys. Chem. B* **1998**, *102*, 2519−2522.
(39) Gupta, S.; Fierro, C.; Yeager, E. *J. Electroanal. Chem.* **1991**, *306*, 239−250.
(40) von Deak, D.; Singh, D.; King, J. C.; Ozkan, U. S. *Appl. Catal., B* **2011**, *113−114*, 126−133.
(41) von Deak, D.; Singh, D.; Biddinger, E. J.; King, J. C.; Bayram, B.; Miller, J. T.; Ozkan, U. S. *J. Catal.* **2012**, *285*, 145−151.
(42) Singh, D.; King, J. C.; Ozkan, U. Modified carbon materials as O_2 reduction reaction electrocatalysts in acid PEM fuel cells. In *Non-Noble Metal Fuel Cell Catalysts*; Chen, Z., Dodelet, J. P., Zhang, J., Eds.; Wiley-VCH: New York, 2013; pp 119−141.
(43) Lefevre, M.; Proietti, E.; Jaouen, F.; Dodelet, J.-P. *Science* **2009**, *324*, 71−74.
(44) Biddinger, E. J.; Knapke, D. S.; von Deak, D.; Ozkan, U. S. *Appl. Catal., B* **2010**, *96*, 72−82.
(45) Yu, X.-g.; Xie, J.-y.; Yang, J.; Huang, H.-j.; Wang, K.; Wen, Z.-s. *J. Electroanal. Chem.* **2004**, *573*, 121−128.
(46) Contamin, O.; Debiemme-Chouvy, C.; Savy, M.; Scarbeck, G. *J. New Mater. Electr. Sys.* **2000**, *3*, 67−74.
(47) Wang, X.; Zheng, W. T.; Tian, H. W.; Yu, S. S.; Xu, W.; Meng, S. H.; He, X. D.; Han, J. C.; Sun, C. Q.; Tay, B. K. *Appl. Surf. Sci.* **2003**, *220*, 30−39.
(48) Ganesan, S.; Leonard, N.; Barton, S. C. *Phys. Chem. Chem. Phys.* **2014**, *16*, 4576−4585.
(49) Descostes, M.; Mercier, F.; Thromat, N.; Beaucaire, C.; Gautier-Soyer, M. *Appl. Surf. Sci.* **2000**, *165*, 288−302.
(50) Pu, M.; Ma, Y.; Wan, J.; Wang, Y.; Huang, M.; Chen, Y. *J. Colloid Interface Sci.* **2014**, *418*, 330−337.
(51) Zhong, W. H.; Tay, B. K.; Lau, S. P.; Sun, X. W.; Li, S.; Sun, C. Q. *Thin Solid Films* **2005**, *478*, 61−66.
(52) Wanga, X.; Zhenga, W. T.; Tiana, H. W.; Yua, S. S.; Xua, W.; Mengb, S. H.; Heb, X. D.; Hanb, J. C.; Tayc, C. Q. S. B. K. *Appl. Surf. Sci.* **2003**, *220*, 30−39.
(53) Zhang, L.; Millet, J. M. M.; Ozkan, U. S. *J. Mol. Catal. A: Chem.* **2009**, *309*, 63−70.
(54) Palaniselvam, T.; Kannan, R.; Kurungot, S. *Chem. Commun.* **2011**, *47*, 2910−2912.
(55) O'Day, P. A.; Rivera, N.; Root, R.; Carroll, S. A. *Am. Mineral.* **2004**, *89*, 572−585.
(56) Liu, S.-H.; Wu, J.-R.; Pan, C.-J.; Hwang, B.-J. *J. Power Sources* **2014**, *250*, 279−285.
(57) Bron, M.; Radnik, J.; Fieber-Erdmann, M.; Bogdanoff, P.; Fiechter, S. *J. Electroanal. Chem.* **2002**, *535*, 113−119.
(58) Tsai, C.-W.; Chen, H. M.; Liu, R.-S.; Asakura, K.; Zhang, L.; Zhang, J.; Lo, M.-Y.; Peng, Y.-M. *Electrochim. Acta* **2011**, *56*, 8734−8738.
(59) Kramm, U. I.; Lefevre, M.; Larouche, N.; Schmeisser, D.; Dodelet, J. P. *J. Am. Chem. Soc.* **2014**, *136*, 978−985.